Reviewed

A Search and Shrink Approach for the Baseline Constrained LAMBDA Method: Experimental Results

G. Giorgi, P.J.G. Teunissen, P.J. Buist, *Delft University of Technology*

G.Giorgi@tudelft.nl

BIOGRAPHY

Gabriele Giorgi and Peter Buist are PhD students at the Mathematical Geodesy and Positioning (MGP) group of the Delft Institute of Earth Observation and Space Systems (DEOS). Peter Teunissen is Head of MGP and full professor of Earth Observation and Navigation at the Delft University of Technology. Their research focuses on investigating the capabilities of the next generation GNSS for relative navigation and attitude determination of space platforms.

ABSTRACT

In this paper we present experimental results of a new approach for resolving GNSS baseline constrained integer ambiguities. The method is based on a modification of the LAMBDA method, where the a-priori information on the baseline length is exploited in the search process. The integer ambiguity vector is searched by means of a processing strategy which iteratively reduces the size of the search space, resulting in fast convergence to the sought-for solution. The Search and Shrink strategy is explained and numerical diagnostics are presented to illustrate its performance. Our results are based on simulated as well as on actual GNSS data and focus on single-frequency, single epoch processing, which is considered the most challenging case of GNSS attitude determination.

1 INTRODUCTION

In order to achieve the highest levels of ranging precision with GNSS, the carrier-phase observations must be employed. The carrier-phase measurements are however affected by unknown integer ambiguities, which must be resolved in order to take advantage of the high carrier-phase measurement precision. Once the ambiguities are fixed, the precise data can be used for a wide range of demanding applications, ranging from terrestrial to maritime and aerospace utilizations. An important problem in a wide range of applications is GNSS-based attitude determination, where the baseline length is usually known. For this problem integer ambiguity resolution is still challenging, in particular if one aims at single-frequency, single-epoch GNSS-based attitude determination.

Various approaches have been developed for resolving the GNSS attitude ambiguity resolution problem, see e.g. ([1], [2], [3], [4], [5], [6], [7]). In this contribution we will work with the LAMBDA (Least squares AMBiguity Decorrelation Adjustment) method. This method, originally introduced in [8],[9],[10], is due to its efficiency and optimality widely used for GNSS ambiguity resolution. The theoretical proof of its optimality was given in [11].

The standard LAMBDA method can be applied to all unconstrained and linearly constrained GNSS models. In case of nonlinear constraints an extension is needed. Such an extension is the baseline constrained LAMBDA method as introduced in [12] for the GNSS compass problem. Practical results obtained with this method can be found in e.g. ([13], [14], [15], [16], [17], [18], [19]). In this method different options exist for setting the size of the search space and for performing the actual search. It is the presence of the baseline length constraint that makes the setting of an adequate search space size particularly challenging. One option for setting the size of the search space is based on setting a tight initial size possibly followed by incremental inflations in case the search space is found empty. Although the size of the incremental inflations are chosen a priori, this approach has shown to result in a very efficient search. This approach and results obtained with it are described in [13] and [19].

Another option for handling the size of the search space and the search in it, is based on the so-called Search and Shrink approach as introduced in [20]. With this approach it is guaranteed that one starts with a nonempty search space. This initial space may be too large however for an exhaustive search. A partial search followed by a shrinkage step is therefore applied until the sought for integer minimizer is found. It is this Search and Shrink approach of the baseline constrained LAMBDA method that we will study in the present contribution.

This contribution is structured as follows. In Section 2 we introduce the models for the unconstrained and constrained integer least squares problem, while Section 3 gives a brief review of the LAMBDA method. In Sec-

tion 4 we present elements of the constrained LAMBDA method and briefly describe its Search and Shrink strategy. The performance of this strategy is studied in the sections following. In Section 5 results are presented which are obtained from simulated data, while in Section 6 results are reported that are obtained from actual data of a static ground station and of a dynamic antenna-frame mounted onboard an aircraft.

2 INTEGER LEAST SQUARES

The system of linearized double differences code and carrier phase observations can be expressed as

$$E(y) = Aa + Bb \quad D(y) = Q_y \quad (1)$$

where $E(.)$ and $D(.)$ are the expectation and dispersion operator, respectively, y is the vector of observables, a is the vector of ambiguities, and b is the baseline vector. A is the matrix containing the carrier wavelengths, B is the matrix containing the line of sight vectors, and Q_y is the variance-covariance matrix of the observables. In this formulation we neglect the atmospheric errors, limiting our analysis to short baseline applications.

The least-squares minimization problem of model (1) reads

$$\min_{a,b} \|y - Aa - Bb\|^2_{Q_y} \quad a \in \mathbb{Z}^n, b \in \mathbb{R}^3 \quad (2)$$

Since it is subject to the integer constraints on the carrier phase ambiguities, $a \in \mathbb{Z}^n$, it has been coined an *Integer Least Squares* (ILS) problem in [8].

In our present application we have one additional constraint, namely that the length of the baseline vector is known, $\|b\| = l$. Our least-squares minimization problem becomes then

$$\min_{a,b} \|y - Bb - Aa\|^2_{Q_y} \quad a \in \mathbb{Z}^n, b \in \mathbb{R}^3, \|b\|^2 = l^2 \quad (3)$$

This least-squares problem has been coined a *Quadratically Constrained Integer Least-Squares* (QC-ILS) problem in [20].

3 THE LAMBDA METHOD

We first briefly discuss the LAMBDA method for solving (2). The method is based on the following orthogonal decomposition [21]:

$$\|y - Aa - Bb\|^2_{Q_y} = \|\hat{e}\|^2_{Q_y} + \|\hat{a} - a\|^2_{Q_{\hat{a}}} + \|\hat{b}(a) - b\|^2_{Q_{\hat{b}(a)}} \quad (4)$$

where $\hat{e} = y - A\hat{a} - B\hat{b}$ is the residual vector, $\hat{a}$ and $\hat{b}$ are the float ambiguity and float baseline solution, respectively, and $\hat{b}(a)$ is the conditional baseline solution. The float solutions $\hat{a}$ and $\hat{b}$ are computed from the normal equations

$$\begin{bmatrix} A^T Q_y^{-1} A & A^T Q_y^{-1} B \\ B^T Q_y^{-1} A & B^T Q_y^{-1} B \end{bmatrix} \begin{bmatrix} \hat{a} \\ \hat{b} \end{bmatrix} = \begin{bmatrix} A^T Q_y^{-1} y \\ B^T Q_y^{-1} y \end{bmatrix} \quad (5)$$

Since the third term on the right side of (4) can be made zero for any $a \in \mathbb{Z}^n$, the solution to our minimization problem is given as

$$\check{a} = \arg \min_{a \in \mathbb{Z}^n} \|\hat{a} - a\|^2_{Q_{\hat{a}}} \quad , \quad \check{b} = \hat{b}(\check{a}) \quad (6)$$

The computation of $\check{a}$ is a nontrivial task which involves a discrete search strategy. The search space is defined as

$$\Omega_0 \left(\chi^2 \right) = \left\{ a \in \mathbb{Z}^n \mid \|\hat{a} - a\|^2_{Q_{\hat{a}}} \leq \chi^2 \right\} \quad (7)$$

Geometrically, the search space is an ellipsoid in an n-dimensional space, centred at $\hat{a}$ and with its size governed by the positive constant χ^2. Note that χ^2 must be chosen large enough to guarantee the presence of the integer minimizer, but not too large to avoid a too high computational load. Considerations on the importance in the choice of χ^2 can be found in [22] and [23]. Experience has shown that the use of the bootstrapped solution is often a good choice for setting the initial search space.

In case of GNSS the ambiguity search space (7) usually has a significant elongation due to the covariance properties of the double differenced ambiguities [21]. As a result, the search for the integer minimizer $\check{a}$ will usually become highly inefficient. The LAMBDA method takes care of this by means of a decorrelation of the float ambiguities that is realized via an integer preserving transformation matrix. As a result, the search becomes much faster in the decorrelated space and the computation of the integer minimizer much more efficient.

4 THE CONSTRAINED LAMBDA METHOD

The baseline constrained model (3) is solved by modifying the original LAMBDA method whereby knowledge of the baseline length, $\|b\| = l$, is exploited both in the derivation of the float solution and in the search process.

4.1 Quadratically constrained integer least-squares

It follows from (4) that

$$\min_{a \in \mathbb{Z}^n, b \in \mathbb{R}^3, \|b\| = l} \|y - Aa - Bb\|^2_{Q_y} = \|\hat{e}\|^2_{Q_y} +$$
$$\min_{a \in \mathbb{Z}^n} \left(\|\hat{a} - a\|^2_{Q_{\hat{a}}} + \min_{b \in \mathbb{R}^3, \|b\| = l} \|\hat{b}(a) - b\|^2_{Q_{\hat{b}(a)}} \right) \quad (8)$$

Note that now the third term on the right hand side does not vanish due to the baseline length constraint.
If we define

$$F(a) = \|\hat{a} - a\|^2_{Q_{\hat{a}}} + \|\hat{b}(a) - \check{b}(a)\|^2_{Q_{\hat{b}(a)}} \quad (9)$$

with

$$\check{b}(a) = \arg \min_{b \in \mathbb{R}^3, \|b\| = l} \|\hat{b}(a) - b\|^2_{Q_{\hat{b}(a)}} \quad (10)$$

then the sought for QC-ILS solution is given as

$$\check{a} = \arg \min_{a \in \mathbb{Z}^n} F(a) \quad , \quad \check{b} = \check{b}(\check{a}) \quad (11)$$

Note, due to the presence of the baseline term in $F(a)$, that $\breve{a}$ is now not anymore the integer vector closest to $\hat{a}$. In the above expressions for $\breve{a}$ and $\breve{b}$, the *unconstrained* float solutions $\hat{a}$ and $\hat{b}$ are used. It is also possible however to make use of the *baseline constrained* float solutions. As shown in [12] this is achieved by replacing $\hat{a}, \hat{b}(a), Q_{\hat{a}}$ and $Q_{\hat{b}(a)}$ in (9) and (10) by their constrained counterparts.

4.2 An exhaustive search

In principle the solution $\breve{a}$ of (11) can be computed by means of an exhaustive search in the search space

$$\Omega\left(\chi^2\right) = \left\{a \in \mathbb{Z}^n \mid F(a) \leq \chi^2\right\} \qquad (12)$$

First one collects all integer vectors that lie inside $\Omega\left(\chi^2\right)$ and from this set one then selects the integer vector that returns the smallest value for $F(a)$. Note however that the search space is no longer an ellipsoid as it was in the unconstrained case. This complicates the search somewhat. As a remedy one can work with an ellipsoidal search space that encompasses $\Omega\left(\chi^2\right)$. The steps for computing $\breve{a}$ are then as follows:

1. Set the size of the search space by taking $\tilde{\chi}^2 = F(\tilde{a})$ for some $\tilde{a} \in \mathbb{Z}^n$. For a discussion on the choice of $\tilde{a}$ see Section 5.3.

2. Enumerate all the integer vectors contained in the larger (ellipsoidal) search space (see Fig.1)

$$\Omega_0\left(\tilde{\chi}^2\right) = \left\{a \in \mathbb{Z}^n \mid \|\hat{a} - a\|_{Q_{\hat{a}}}^2 \leq \tilde{\chi}^2\right\} \supseteq \Omega\left(\tilde{\chi}^2\right)$$

   This can be efficiently performed with the LAMBDA method.

3. Compute $F(a)$ for each collected integer vector and select the one which returns the smallest value for this objective function.

Clearly this exhaustive search is simple and rather straightforward to apply. However, it also has the tendency of being rather inefficient, in particular if the underlying GNSS model lacks sufficient strength. Since $F(a)$ needs to be
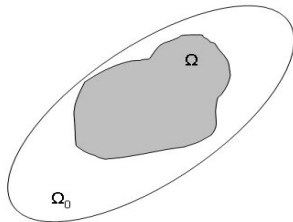

Fig. 1: Visualization of the sets $\Omega(\chi^2)$ and $\Omega_0(\chi^2)$.

computed for all integer candidates, this also holds true for the rather time-consuming computation of $\breve{b}(a)$, c.f. (10). Hence, the whole search becomes very inefficient if the search space contains too many integer vectors. This can be avoided if one is in the position of computing a small enough value for $\tilde{\chi}^2$, which is possible if the underlying GNSS model has sufficient strength. This is the case for example with short-baseline multi-frequency models, where the bootstrapped solution (or even the rounded one) based on the unconstrained float solution is already close to the final fixed solution. It is generally not the case however for models based on single-frequency, single-epoch data.

4.3 Search and Shrink

To make the search much more efficient a Search and Shrink strategy was introduced in [20]. It aims at iteratively reducing the size of the search space without the necessity of computing $\breve{b}(a)$ at each step. An important element of this new approach lies in its capacity of bounding the function $F(a)$ by functions that are easier to evaluate.

If we make use of the maximum (λ_{max}) and the minimum (λ_{min}) eigenvalues of the matrix $Q_{\hat{b}(a)}^{-1}$, we can construct the followings inequalities:

$$F_1(a) \leq F(a) \leq F_2(a)$$

$$F_1(a) = \|\hat{a} - a\|_{Q_{\hat{a}}}^2 + \lambda_{min}\left(\|\hat{b}(a)\|_{I_3} - l\right)^2 \qquad (13)$$

$$F_2(a) = \|\hat{a} - a\|_{Q_{\hat{a}}}^2 + \lambda_{max}\left(\|\hat{b}(a)\|_{I_3} - l\right)^2$$

With the two functions $F_1(a)$ and $F_2(a)$ correspond the following two search spaces

$$\Omega_1\left(\chi^2\right) = \left\{a \in \mathbb{Z}^n \mid F_1(a) \leq \chi^2\right\}$$
$$\Omega_2\left(\chi^2\right) = \left\{a \in \mathbb{Z}^n \mid F_2(a) \leq \chi^2\right\} \qquad (14)$$

Note that (see Fig.2)

$$\Omega_2(\chi^2) \subseteq \Omega(\chi^2) \subseteq \Omega_1(\chi^2) \qquad (15)$$

In short the algorithm now works as follows. We first determine the integer minimizer of $F_2(a)$ by means of a Search and Shrink strategy. Starting with a certain initial χ_0^2, we search for an integer vector in the (decorrelated) space Ω_2:

$$\Omega_2\left(\chi_0^2\right) = \left\{a \in \mathbb{Z}^n \mid F_2(a) \leq \chi_0^2\right\} \subseteq \Omega\left(\chi_0^2\right) \qquad (16)$$

As soon as such an integer vector is found, say $\tilde{a}$, the space is shrunk to the value $\tilde{\chi}^2 = F_2(\tilde{a}) < \chi_0^2$ and the search continues in this smaller set. In this way the search proceeds rather quickly towards the integer minimizer of $F_2(a)$, which we denote as $\breve{a}_2$. This integer vector is not necessarily the minimizer of $F(a)$, but it is known to lie inside the set

$$\Omega\left(\chi_1^2\right) \subseteq \Omega_1\left(\chi_1^2\right) = \left\{a \in \mathbb{Z}^n \mid F_1(a) \leq \chi_1^2\right\} \qquad (17)$$
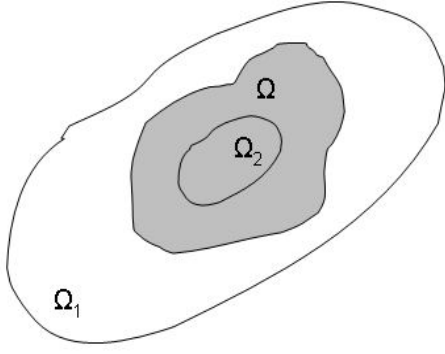
Fig. 2: Visualization of $\Omega(\chi^2)$ and its two bounding sets $\Omega_1(\chi^2)$ and $\Omega_2(\chi^2)$.

with $\chi_1^2 = F_2(\breve{a}_2)$. All the integer vectors contained in Ω_1 are then enumerated and the integer minimizer of $F(a)$ is selected.

The search algorithm is thus divided in three consecutive steps: shrinking (working with the set Ω_2), enumerating (working with the set Ω_1) and minimizing (computing $F(a)$ for the remaining candidates). Fig.3 illustrates the flow chart of the algorithm. For a detailed description of the Search and Shrink strategy we refer to [20].

5 SIMULATION RESULTS
5.1 Simulation set up

Date and time	22 Jan 2008 00:00
Location	Lat: 50° , Long:3°
GPS week	439
Scenario	Single baseline, stationary
Frequency	L1
Number of Satellite vs PDOP	
5	4.192
6	2.142
7	1.917
8	1.811
Undifferenced code noise	
$\sigma_p \; [cm]$	30 - 15 - 5
Undifferenced phase noise	
$\sigma_\phi \; [mm]$	30 - 3 - 1
Baseline length l	2.00 m
Epochs simulated	10^5
Convention on the figures: $pp \_ cc$	
pp: code noise in cm	
cc: phase noise in mm	

Table 1: Simulation set up.

In order to investigate the performance of the algorithm, we first tested it on simulated data. Table 1 reports the
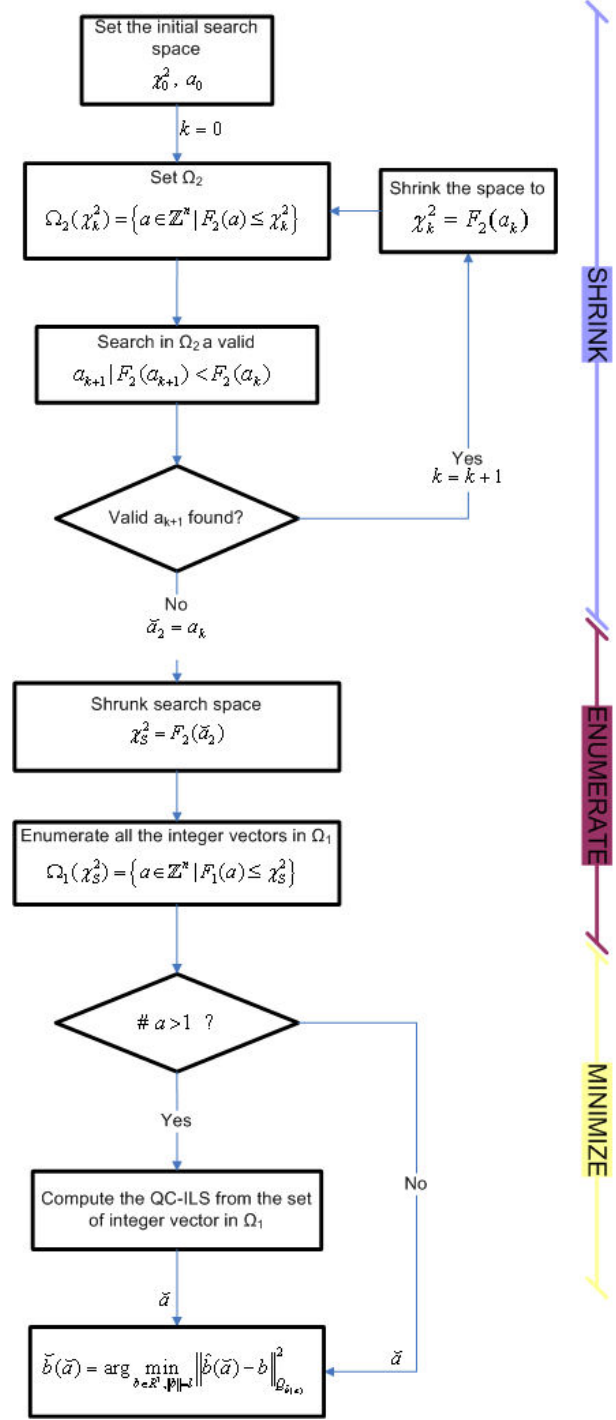

Fig. 3: Flow chart of the Search and Shrink algorithm.

conditions of the simulations. Via the software VISUAL [24], based on a certain location of the receivers and the actual GPS constellation, the design matrices of model (1) were build. Assuming different levels of noise on the undifferenced phase (from 1 mm to 30 mm) and un-

differenced code (from 5 cm to 30 cm) data, a set of 10^5 data was generated randomly for every combination; then each simulation was repeated for different number of satellites varying between 5 and 8, corresponding to different PDOP values. Other sources of error, such as multipath, have not been considered here, to test the algorithm in a controlled environment, with limited sources of error. Later on, we processed experimental datasets, to properly challenge the method in real environments, ranging from high quality-static scenario (ground station, see Section 6.1) to high-dynamic platforms (aircraft, see Section 6.1). Two different aspects have been investigated: the experimental success rate, which depends on the strength of the underlying GNSS model, and the speediness of the method, which is mainly related to the search strategy adopted.

5.2 Single-frequency, single-epoch success rates

The experimental success rate is defined as the percentage of occurrences wherein the true integer vector has been correctly fixed among the total number of epochs processed. Table 2 shows unconstrained and constrained LAMBDA success rates for a 2m baseline in dependence of the number of satellites tracked and the phase and code level noise (σ_ϕ, σ_p).

The baseline constrained LAMBDA method clearly provides much better results than its unconstrained version. The differences in success rate are particularly pronounced when the strength of the underlying GNSS model becomes weaker (fewer satellites and/or higher measurement noise). Making use of the baseline constraint in these cases improves the success rate considerably. According to Table 2 already 5 satellites and a phase standard deviation of 3 mm gives a higher than 70% success rate. The differences in success rate become less pronounced when the strength of the underlying GNSS model increases. For instance, with 8 satellites and a phase and code precision of 3 mm and 5 cm, respectively, a close to 100% success rate is already achieved with the standard LAMBDA method.

5.3 Computational timing

A fundamental aspect for GNSS ambiguity resolution is the speed with which the various computations can be performed. This is particularly relevant for applications that require (near) real-time results.

Setting the size of the search space

It is important to be able to set the size of the search space at an appropriate level, i.e. not too small and not too large. A too small size results in an empty search space, while a too large size results in a search space with an abundance of integer vectors in it. To guarantee that the search space is nonempty and thus includes the sought for integer minimizer, we set the size of the search space by taking $\tilde{\chi}^2 = F_2(\tilde{a})$ for some $\tilde{a} \in \mathbb{Z}^n$. We studied four different ways of choosing such $\tilde{a}$:

- Rounding the unconstrained float solution ($R1$),

- Rounding the constrained float solution ($R2$),

- Bootstrapping the constrained float solution, using $Q_{\hat{a}}^{-1}$ as weight matrix, ($B1$),

- Bootstrapping the constrained float solution, using the Hessian matrix of $F_2(a)$ as weight matrix, ($B2$).

In all these four cases we first applied a decorrelating Z-transformation before rounding or bootstrapping was done. To show how close the timing performance of the constrained LAMBDA Search and Shrink strategy is to the timing performance of the standard LAMBDA method, the timing results are shown in Fig.4 as a ratio with respect to the standard LAMBDA timing results. Since the complexity of the constrained LAMBDA method is larger than that of the standard LAMBDA method, one can expect the former to be slower than the latter. Furthermore, the code for the constrained LAMBDA algorithm has not been optimized yet.

σ_ϕ [mm]		30			3			1	
σ_p [cm]	30	15	5	30	15	5	30	15	5
N	*Success rate, standard LAMBDA*								
	Success rate, constrained LAMBDA								
5	0.41	2.84	29.59	3.30	19.50	86.67	5.99	26.89	95.37
	3.47	9.57	41.64	72.43	88.86	**99.63**	96.54	**99.94**	**100**
6	0.64	3.54	30.95	24.83	66.71	96.89	49.13	86.67	**99.99**
	4.31	12.17	43.51	95.75	**99.18**	**99.90**	**99.99**	**100**	**100**
7	0.83	4.40	34.08	50.24	79.69	**99.53**	74.17	93.27	**100**
	5.80	14.41	46.34	**99.34**	**99.97**	**100**	**100**	**100**	**100**
8	1.09	5.68	36.10	86.17	94.48	**99.99**	**99.972**	**99.99**	**100**
	6.78	17.13	47.75	**99.80**	**99.99**	**100**	**100**	**100**	**100**

Table 2: Simulation results: single-frequency, single-epoch success rates (in %) for the unconstrained and constrained LAMBDA methods. Success rates higher than 99% have been stressed.

The overall results of Fig.4 show however that the differences are not too large, in particular if one focuses on the cases for which the constrained LAMBDA success rates are larger than 99% (see Table 2).

As to the choice of setting the search space size, the results show that rounding the constrained float solution ($R1$) and bootstrapping the constrained float solution, using the Hessian matrix as weight matrix ($B2$), give the best overall timing performance.
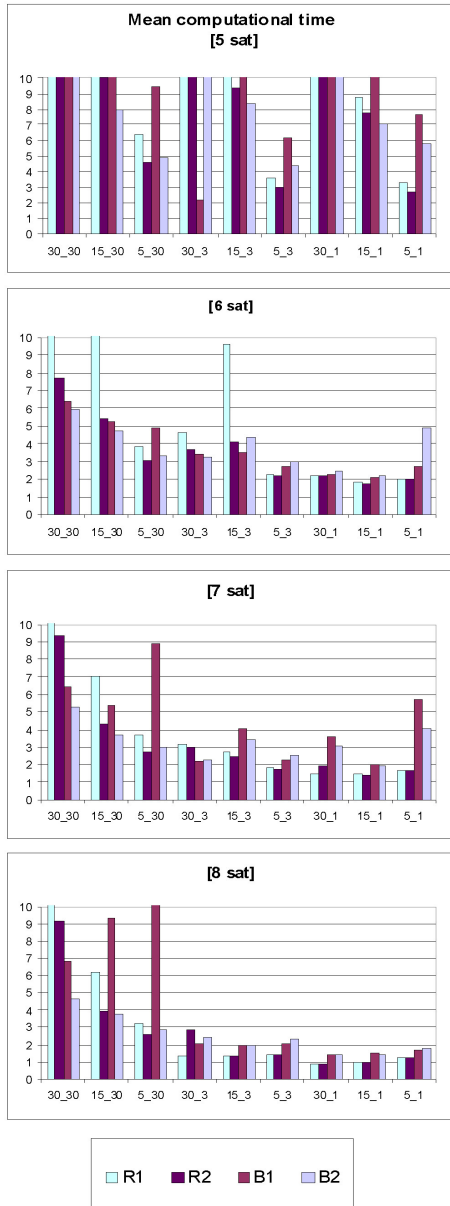

Fig. 4: Ratios with respect to standard LAMBDA of the mean computational search times for four different ways of setting the size of the initial search space: $R1, R2, B1, B2$.
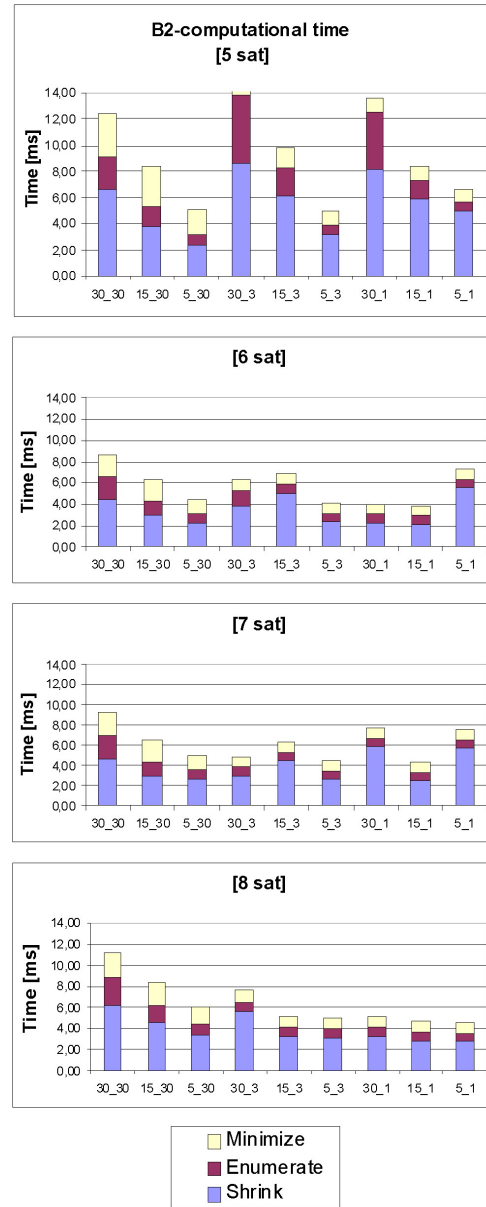

Fig. 5: Mean computational time: division between the three steps of the baseline constrained LAMBDA algorithm. Setting the size of the initial search space: B2

Distribution of computational load

Fig.5 shows how the (mean) computational time is distributed over the 3 different steps of the algorithm (shrink Ω_2, enumerate Ω_1, and minimize $F(a)$). In all cases the size of the search space has been set by bootstrapping using the Hessian ($B2$). To make the comparison proper, we remark that the computation of the integer minimizer has been included also when only one integer vector was con-

Nsat		5	6	7	8
σ_ϕ [mm]	σ_p [cm]	Maximum and mean number of enumerated integer vectors			
30	30	64	25	28	31
		4.50	2.36	2.51	2.59
	15	34	22	35	30
		4.01	2.28	2.36	2.33
	5	22	10	11	13
		2.23	1.44	1.44	1.55
3	30	32	8	14	6
		2.41	1.08	1.02	1.01
	15	21	7	4	4
		1.77	1.03	1.01	1.01
	5	9	2	1	1
		1.11	1.01	1	1
1	30	11	2	1	1
		1.13	1.01	1	1
	15	6	1	1	1
		1.01	1	1	1
	5	2	1	1	1
		1.01	1	1	1

Table 3: Simulation results: maximum and mean number of enumerated integer vectors in the shrunk space.

Baseline	l [m]	Success rate %	Computational time Mean [ms]
		Standard LAMBDA	
A-B	2.20	99.99	3.9
A-R7	2.21	99.80	4.0
B-R7	1.74	99.67	4.1
		Constrained LAMBDA	
A-B	2.20	100	7.4
A-R7	2.21	100	6.9
B-R7	1.74	100	7.2

Table 4: Single-frequency, single-epoch success rates (%) and $B2$-based computational times for the ground station.

6.1 Ground station

The reference station was set up placing an antenna (Trimble Zephyr Geodetic L1/L2) above a known static reference point; two other antennas (Trimble Geodetic W Groundplane) were then placed in proximity of the first one at a known fixed distance (see Table 4). The three antennas were connected to a Trimble R7 and two Trimble SSi (A and B) receivers. Data were collected between 10:44 and 13:29, UTC time, for a total of 9915 epochs logged. The number of satellites tracked equaled 9 most
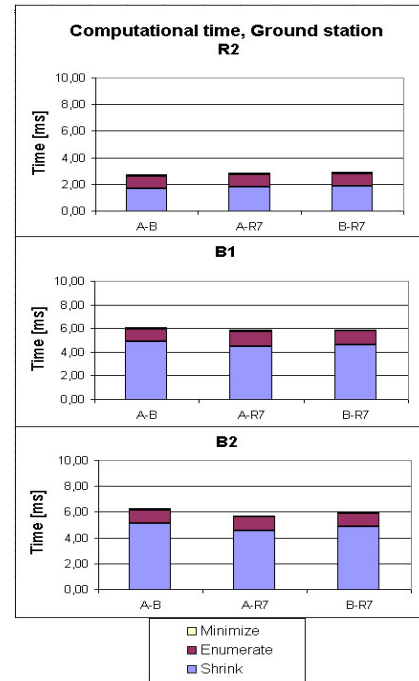
tained in the shrunk search space. The results show that the enumeration- and minimization step take the shortest time, while the shrinking process generally accounts at least for 60% of the total computational time. That the enumeration and minimization can be done so quickly is in fact due to the successful performance of the shrinking process. It is the shrinking that allows one to finally work with so small search spaces.

To illustrate the success of the shrinking process, Table 3 shows the number of enumerated integer vectors in the shrunk search space for different number of tracked satellites and varying noise on the code and phase observations. It shows that the number of integer vectors inside the shrunk search space is indeed very small in general and that it gets smaller as the strength of the underlying GNSS model gets larger (more satellites and/or lower noise).

6 EXPERIMENTAL RESULTS

To support an aerial remote sensing campaign held on 1 November 2007 in the Netherlands, several GPS antennas/receivers were mounted onboard the TU Delft aircraft. Furthermore, a static ground station was set up by using three receivers and three antennas forming a frame with known geometry. The Search and Shrink approach was tested both on the static set up and the dynamic platform.

Fig. 6: Mean computational time of ground station using rounding constrained solution ($R2$), bootstrapping constrained solution ($B1$), and bootstrapping constrained solution with Hessian ($B2$). The division between shrinking, enumeration and minimization is also shown.

Fig. 7: The Cessna Citation II aircraft of the Faculty of Aerospace Engineering, Delft University of Technology.

Baseline	$l\ [m]$	Success rate %	Computational time Mean $[ms]$
Standard LAMBDA			
bI	4.90	25.08	7.7
bII	7.61	60.54	7.5
Constrained LAMBDA			
bI	4.90	62.38	31.9
bII	7.61	94.00	19.4

Table 5: Single-frequency, single-epoch success rates and $B2$-based computational times for aircraft data.

of the time with a few drops to 8 satellites. The PDOP was around 2 most of the time with a few excursions to values around 3.

Table 4 shows the success rates and the mean computational times obtained with the standard and constrained LAMBDA methods. Note that both methods show the same order of efficiency and that they both produce high success rates, with those of the constrained LAMBDA method being larger of course. The high success rates for the unconstrained case is due to the number of satellites tracked (8 or 9) and the high quality receivers used ($\sigma_\phi = 3$ mm, $\sigma_p = 30$ cm), see also Table 2. The results of Fig.6 confirm our simulated results. Rounding or bootstrapping the constrained solution ($R2,B1$) and bootstrapping the constrained solution using the Hessian of the objective function ($B2$) give good results for setting the size of the search space. Also note that due to the success of the shrinking process almost no time is needed for the minimization. In fact, in the computations of all three baselines the shrinking process resulted in all cases except one in a search space containing only a single integer vector.

6.2 The aircraft

Our experiment was conducted with the Cessna Citation II aircraft of the Faculty of Aerospace Engineering, Delft
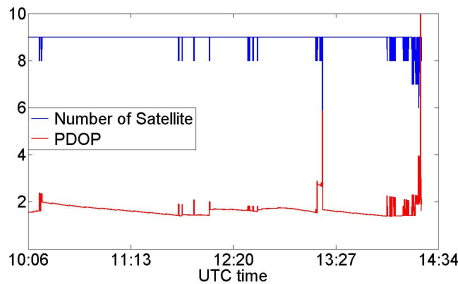
University of Technology (see Fig.7). The aircraft was equipped with three GNSS antennas: one on the body, approximately in the middle of the fuselage (L1/L2 Sensor Systems), one on the wing and one on the nose (both L1 Sensor System). We name bI the body-nose baseline, bII the body-wing baseline. These three antennas were all connected to a Septentrio PolaRx2@, logging data at 10Hz for the entire duration of the flight. Data were collected on 1 November 2007, between 10:06 and 14:23, UTC time, for a total of 154511 epochs logged. Fig.8 shows the number of satellites tracked and corresponding PDOP values.

Table 5 shows the empirical success rates and the mean computational times for both the standard and the constrained LAMBDA method. Note that the aircraft data
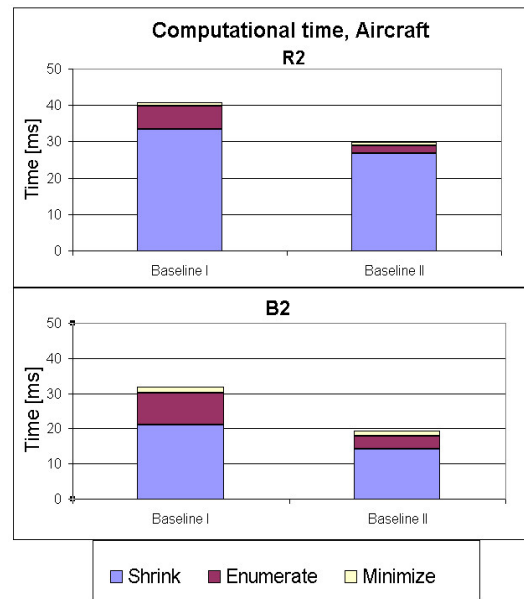

Fig. 8: Number of satellites tracked from aircraft and corresponding PDOP values.

Fig. 9: Mean computational time for aircraft data using rounding constrained solution ($R2$) and bootstrapping constrained solution with Hessian ($B2$). The division between shrinking, enumeration and minimization is also shown.

shows a poorer performance than that of the ground station data (compare with Table 4). The lower success rates can be explained by the higher noise levels in the data and the presence of multipath, in particular on the data of the first baseline. The computational times are still fast, although a bit slower than for the static ground station data, see also Fig.9. Note that the minimization step is still extremely fast. This is due to the low number of integer vectors that remain in the shrunken search space. The number of enumerated integer vectors contained in the shrunken search space is shown in Fig.10. The maximum number of integer vectors is lower than 23, while in most of the cases only a single integer vectors remains (first baseline: 80% and second baseline: 90%).
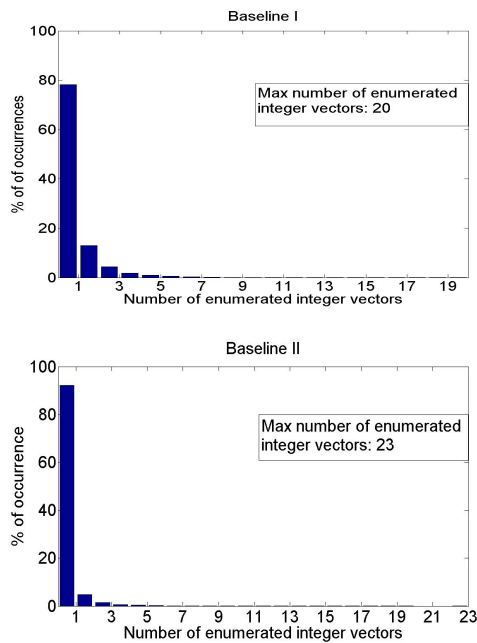

Fig. 10: Number of enumerated integer vectors in the shrunken search space for baselines I and II of the aircraft data.

7 CONCLUSIONS

The constrained LAMBDA method exploits the a priori knowledge of the baseline length l. This leads to a new objective function for finding the integer least-squares ambiguities. This objective function not only weighs by how much the float ambiguity solution differs from an integer vector, but also by how much the integer ambiguity constrained baseline solution differs from a sphere with radius l. Different strategies can be followed for finding the integer minimizer of the new objective function [12], [13], [19], [20].

In this contribution we presented experimental results of

the Search and Shrink strategy as introduced in [20]. This strategy works with bounding functions of the objective function that are easy to evaluate and it uses an iterative scheme to shrink the search space. In this way the search proceeds quickly toward the integer minimizer of the objective function.

In order to test the method, we processed both simulated and real data (static and dynamic), focusing on the most challenging scenario, being single-frequency (L1), single-epoch GNSS attitude determination. The inclusion of the baseline constraint shows dramatic improvements in the success rates. For most of the measurement scenarios, static as well as dynamic, the constrained LAMBDA method achieves larger than 90% success rates for single-frequency, single epoch data. The presence of severe multipath however can reduce the success rates considerably. As to the efficiency of the method, the shrinking process showed to be very successful indeed in all cases treated. By means of shrinking it was achieved that only a limited number of integer vectors, often only one, had to be enumerated to find the sought-for minimizer.

REFERENCES

[1] P Montgomery I Y Bar-Itzhack and J Garrick. Algorithm for Attitude Determination using GPS. *Proceedings of AIAA Guidance, Navigation and Control Conf., New Orleans, LA, USA. Aug. 1997, Paper no. AIAA 97- 3616*, 1997.

[2] C E Cohen. Attitude Determination Using GPS. 1992.

[3] G Lu. Development of a GPS Multi-antenna System for Attitude Determination. *UCGE Reports 20073, Dept. of Geomatics Eng., University of Calgary*, 1995.

[4] C Park, I Kim, J G Lee, and G I Jee. Efficient Ambiguity Resolution Using Constraint Equation. *Proceedings of IEEE: Position, Location and Navigation Symposium PLANS96, Atlanta, Georgia, USA*, 1996.

[5] C Park, I Kim, J G Lee, and G I Jee. Efficient Technique to Fix GPS Carrier Phase Integer Ambiguity On-the-fly. *Proceedings of IEEE: Radar, Sonar and Navigation, Vol. 144, No. 3*, 1997.

[6] C H Tu, K Y Wang, and W C Melton. GPS Compass: A Novel Navigation Equipment. *Proceedings*

of ION National Technical Meeting, Santa Monica, CA, USA, 1996.

[7] M Ziebart and P Cross. LEO GPS Attitude Determination Algorithm for a Macro-satellite Using Boom-arm Deployed Antennas. *GPS Solutions, 6:242-256*, 2003.

[8] P J G Teunissen. Least Squares Estimation of the Integer GPS Ambiguities. *Invited lecture, Section IV Theory and Methodology, IAG General Meeting, Beijing*, 1993.

[9] P J G Teunissen. A New Method for Fast Carrier Phase Ambiguity Estimation. *Proceedings IEEE Position Location and Navigation Symposium, PLANS '94*, pages 562–573, 1994.

[10] P J G Teunissen. The Least-Squares Ambiguity Decorrelation Adjustment: a Method for Fast GPS Integer Ambiguity Estimation. *Journal of Geodesy*, 70:65–82, 1995.

[11] P J G Teunissen. An Optimality Property of the Integer Least-Squares Estimator. *Journal of Geodesy*, 73(11):587–593, 1999.

[12] P J G Teunissen. The LAMBDA Method for the GNSS Compass. *Artificial Satellites, Vol.41,N.3*, 2006.

[13] C Park and P J G Teunissen. A New Carrier Phase Ambiguity Estimation for GNSS Attitude Determination Systems. *Proceedings of International GPS/GNSS Symposium, Tokyo*, 2003.

[14] P Buist. The Baseline Constrained LAMBDA Method for Single Epoch, Single Frequency Attitude Determination Applications. *Proceedings of ION GPS-2007*, 2007.

[15] Y Moon and S Verhagen. Integer Ambiguity Estimation and Validation in Attitude Determination Environments. *Proceedings of the 19th International Technical meeting of the Institute of Navigation Satellite Division, ION GNSS 2006*, pages 335–344, 2006.

[16] L V Kuylen, P Nemry, F Boon, A Simsky, and J F M Lorga. Comparison of Attitude Performance for Multi-Antenna Receivers. *European Journal of Navigation*, 4(2), 2006.

[17] C Hide and D J Pinchin. Development of a Low Cost Multiple GPS Antenna Attitude System. *Proceedings ION GNSS 2007,88-95*, 2007.

[18] J Pinchin, C Hide, D Park, and X Q Chen. Precise Kinematic Positioning Using Single Frequency GPS Receivers and an Integer Ambiguity Constraint. *Proceedings of IEEE PLANS 2008*, 2008.

[19] C Park and P J G Teunissen. A Baseline Constrained LAMBDA Method for Integer Ambiguity Resolution of GNSS Attitude Determination Systems. *Journal of Control, Robotics and Systems (in Korean), 14(6), 587-594*, 2008.

[20] P J G Teunissen. Integer Least Squares Theory for the GNSS Compass. *Journal of Geodesy, Springer, submitted*, 2008.

[21] P J G Teunissen and A Kleusberg. GPS for Geodesy. *Springer, Berlin Heidelberg New York*, 1998.

[22] P J G Teunissen, P J De Jonge, and C C J M Tiberius. The Volume of the GPS Ambiguity Search Space and its Relevance for Integer Ambiguity Resolution. *Proc. of ION GPS-1996, Kansas City MO*, pages 889–898, 1996.

[23] C C J M Tiberius P J De Jonge and P J G Teunissen. Computational aspects of the LAMBDA method for GPS ambiguity resolution. *Proc. of ION GPS-1996, Kansas City MO, pages 935-944*, 1996.

[24] S Verhagen. Visualization of GNSS-related design parameters: Manual for the Matlab user interface VISUAL, 2006.